ARTICLE

Decorating Parylene-Coated Glass with ZnO Nanoparticles for Antibacterial Applications: A Comparative Study of Sonochemical, Microwave, and Microwave-Plasma Coating Routes

G. Applerot,[†,‡] R. Abu-Mukh,[†,‡] A. Irzh,[†,‡] J. Charmet,[§] H. Keppner,[§] E. Laux,[§] G. Guibert,[§] and A. Gedanken*[,‡]

Department of Chemistry, Kanbar Laboratory for Nanomaterials, Institute of Nanotechnology and Advanced Materials, Bar-Ilan University, Ramat-Gan 52900, Israel, and Institut des Microtechnologies Appliquées, University of Applied Sciences (HES-SO) Arc, Eplatures-Grises, 1 7 2300 La Chaux-de Fonds, Switzerland

ABSTRACT A glass substrate, coated with a Parylene film, was coated with ZnO by three different methods: ultrasound, microwave, and microwave-plasma irradiation. These coating modes are simple, efficient, and environmentally friendly one-step processes. The structure of the coated products was characterized and compared using methods such as XRD, HR-SEM, EDS, RBS, and optical spectroscopy. Coating by ZnO nanoparticles was achieved for all three approaches. The products were found to differ in their particle sizes, coating thickness, and depth of penetration. All of the ZnO−Parylene−glass composites demonstrated a significant antibacterial activity against *Escherichia coli* (Gram negative) and *Staphylococcus aureus* (Gram positive) strains.

KEYWORDS: ZnO nanoparticles • Parylene • biomedical coatings

INTRODUCTION

Zinc oxide (ZnO) has been the topic of high-standard contemporary research because of its wide band gap (3.37 eV) and large exciton-binding energy (60 meV), which cause interesting luminescent, piezoelectric, and photoconducting properties (1). These properties make ZnO a technologically important material. This material is suitable for many industrial applications in fields such as high frequency surface devices, as well as for optical devices. ZnO nanoparticles offer considerable potential as a starting material for such applications and for other purposes such as transparent UV-protection films, chemical sensors, LDs, and LEDs, all of which are attracting the attention of increasingly more research groups (2).

Ceramic powders of metal oxides such as ZnO, as well as magnesium oxide (MgO), were found to exhibit marked antibacterial activity (3). Our previous study has established that ZnO can generate some species of oxyradicals in its suspension (4). These reactive oxygen species (ROS) were detected in electron spin resonance (ESR) studies conducted with and without the bacteria present in the ESR tube. However, ZnO is generally regarded as a safe material for human beings and animals, and it has been used extensively in the formulation of personal care products.

The rapid development of different methods for the fabrication and deposition of nanomaterials on polymer and glass surfaces significantly enhanced their application in electronic devices and biotechnology. Recently, some low-temperature methods for the deposition of nanoparticles on a glass substrate were reported, e.g., electrodes plating of spin-coated nanoparticles and deposition of nanoparticles on modified glass slides (5, 6). However, as the utilization of chemicals leads to environmental concerns, other approaches that concur with simplicity and are environmentally friendly are called for. Both sonochemical and microwave irradiation fulfill this requirement and are regarded as "green" chemistry approaches.

Sonochemical methods have been proven as an effective technique for the deposition of nanomaterials on polymeric matrices because of their ability to combine the synthesis of various nanomaterials, as well as their deposition on various substrates in a single operation, without the aid of a binder (7). Upon irradiation with high intensity sound or ultrasound, acoustic cavitation usually occurs. Cavitation, the formation, growth, and implosive collapse of bubbles irradiated with sound, is the impetus for sonochemistry (8). In this technique, when the created bubbles collapse near a solid surface, they produce enormous amounts of energy from the conversion of the kinetic energy of the motion of the liquid into heating the contents of the bubble. The compression of the bubbles during cavitation is more rapid than the

* Corresponding author. E-mail: gedanken@mail.biu.ac.il.
Received for review November 25, 2009 and accepted March 18, 2010
† These authors contributed equally to this project.
‡ Bar-Ilan University.
§ University of Applied Sciences (HES-SO) Arc.
DOI: 10.1021/am900825h

Published on Web 04/01/2010

thermal transport, which generates short-lived, localized hot-spot bubbles having temperatures around 5000 K, a pressure of roughly 1000 atm, and heating and cooling rates above 1×10^{10} K/s. Microjets and shock waves are also created during the compression of the bubbles near solid surfaces. These energetic jets throw the as-prepared nanoparticles onto the surface at a very high speed (>100 m/s), causing the nanoparticles to adhere strongly to the solid surface (9).

Microwave irradiation as a heating method in synthetic chemistry has been a very rapidly developing research area. Microwave heating is promising because of its unique effects, such as rapid volumetric heating, higher reaction rates, higher reaction selectivity, higher yields of products, and energy savings, as compared to conventional heating. Moreover, the use of microwave radiation is the method that perhaps requires the smallest investment in equipment, because it can be carried out in a domestic microwave oven. The effect of heating is created by the interaction of the permanent dipole moment of the molecule with a so-called "kitchen frequency" of 2.45 GHz electromagnetic radiation (10). However, only a few reports were found dealing with deposition of nanoparticles by means of microwave (11).

The preparation of zinc oxide nanoparticles on a glass substrate was conducted recently by a new technique called solvent-assisted deposition in plasma (SADIP), which was recently developed at our laboratory (12). The mechanism of nanoparticle formation in the microwave plasma differs from that of a chemical vapor synthesis in a tubular furnace, as the reactants are ionized and dissociated. This also allows lower reaction temperatures. A microwave plasma reaction is simple, easy to manipulate, and compatible with the commonly used impregnation processes (13). Thus, it is expected that a microwave plasma reaction might open the door for the preparation of metal- and metal-oxide nanoparticles and supported metal catalysts. Moreover, this technique also has the key advantage of its ability to coat specific substrates.

Parylene is the trade name for a variety of polyxylylene polymers. It is a transparent high-molecular-weight polymer film (200 000−400 000 g mol^{-1}) with a typical chain length of 2000−4000 units. Parylene film has a low dielectric permittivity and provides excellent chemical and thermal properties. It allows conformal and pinhole-free coatings by using a chemical vacuum deposition process (CVD) based on the vapor-phase pyrolysis of paracyclophane (14). The Parylene coating process is solvent-free and the deposition on the substrate is performed at ambient temperature. Excellent uniformity is achieved for coating thicknesses ranging from hundreds of nanometers up to several tenths of micrometers. These films are commonly used as moisture barrier layers for electronic boards, corrosion-resistant coatings in archival preservation, and as biopassivation coatings in medical implants. Parylene thin film conformal coatings can be deposited on most biomedical devices or substrates (15). Other potential applications for Parylene include waveguides and coatings for optical systems, acoustic matching layers for transducers, MEMS components, such as membranes and channel walls, and low dielectric constant materials for multilevel integrated circuits (IC) (16). The coated substrates or devices are stable and show little or no change in their response characteristics. Additional typical applications are the formation of mandrels, catheters, guide wires, stents, sensors, transducers, and probes (17).

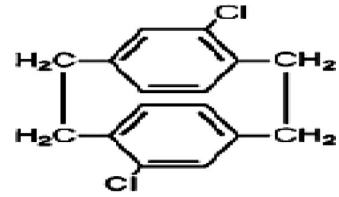

$C_{16}H_8Cl_2$
(Parylene C
repeating unit)

FIGURE 1. Structure of Parylene C.

In the present work, we utilized the three above-mentioned methods for preparing Parylene-coated glass slides with antibacterial properties by immobilizing ZnO nanoparticles on the coated slides. The morphology of the product obtained by the three techniques was characterized by and compared with a complex of physicochemical methods, X-ray diffraction (XRD), high-resolution scanning electron microscopy (HR-SEM), energy-dispersive X-ray spectroscopy (EDS), Rutherford backscattering spectrometry (RBS), and optical spectroscopy studies. Bacteriological tests of the coated glass were carried out with two strains from different species, representative of various bacteria types. *Escherichia coli* (*E. coli*) was used as a model for Gram-negative bacteria and *Staphylococcus aureus* (*S. aureus*) was used as an example for Gram-positive bacteria. To the best of our knowledge, this is the first report on the deposition of zinc oxide nanoparticles on Parylene-coated glass using any of the above-mentioned synthesis techniques, or any other method.

EXPERIMENTAL SECTION

Preparation of Glass-Coated Parylene. Parylene C (Figure 1) deposition was performed in a COMELEC Parylene-Deposition System, model 1010. Parylene films were synthesized under a vacuum (1−7 Pa) by a conventional method (Gorham-Process). Typically, 4 g of Galxyl C (dichloro-[2,2]-paracyclophane), purchased from Galentis, was evaporated at 120 °C and passed through a pyrolization chamber in which dichloro-[2,2]-paracyclophane was thermally cleaved at 650 °C to a reactive monomer. After this pyrolization step, the gas passed through a deposition chamber and the reactive monomers were condensed at 40−60 °C and polymerized at a substrate-surface. Thus, a product of a small layer (~3 μm) of the Parylene C strongly attached onto the glass surface was achieved.

ZnO Deposition Procedures. All the reagents were purchased from Aldrich and were of analytical chemical purity. They were used without additional purification.

Sonochemical Deposition. The ZnO nanoparticles were deposited on a Parylene glass slide by the sonochemical irradiation of Zn^{2+} ion precursors in a water−ethanol solution. This solvent is considered as an environmentally friendly solution. Zinc acetate tetrahydrate $Zn(Ac)_2 \cdot 4H_2O$ was used as a precursor for this reaction. Typically, the zinc acetate was dissolved

in a water:ethanol = 1:9 mixture to obtain a 0.05 M concentration of Zn^{2+} ions. The pH of the solution was adjusted with the addition of ammonia to pH 8. The Parylene glass slide was then inserted into the reactor and sonication was carried out with an immersed Ti-horn (20 kHz, 750 W at 70% efficiency) for a fixed period of time. At the end of the sonochemical reaction, the coated slide was washed with water and ethanol and allowed to dry overnight under a vacuum.

Deposition using Microwave Radiation. A 100 mL flask was loaded with a Parylene glass slide (1 cm ×1 cm), 30 mL of distilled water, 10 mL of ethanol, and 10 mL of poly(ethylene glycol) (M_w = 400 g/mol). The solvent mixture was purged by argon for 30 min to expel the oxygen from the solution. $Zn(Ac)_2$ (0.03M) was completely dissolved in the solution, and the solution became slightly cloudy (other concentrations of $Zn(Ac)_2$ have also been used, results not shown). After the dissolution of the $Zn(Ac)_2$, 0.5 mL of ammonia was added and the solution became more cloudy. The solution was stirred with the addition of more ammonia, until the solution became completely clear. Next, the solution was irradiated by microwaves for 5 min. At the end of the reaction, the Parylene glass slides were washed thoroughly with water and ethanol and then dried overnight under a vacuum. We could detect that the Parylene glass slide underwent modification from a transparent to a white layer.

Deposition using Microwave Plasma: The Reaction System. The reaction system consisted of a domestic microwave oven (900 W) with a drilled hole in the upper part, a plasma chamber made of pyrex, an argon balloon (99.99%), a vacuum pump, and rubber and pyrex pipes that connect the plasma chamber to the argon balloon and to the vacuum pump.

Coating Procedure. Solutions of zinc salts in ethanol with several concentrations have been prepared. A $Zn(NO_3)_2$ solution in ethanol prepared in a 0.03 M concentration and a saturated solution of $Zn(Ac)_2$ in ethanol (~0.03 M) were also prepared. Three drops of the prepared solution were dropped on quadratic Parylene−glass slides of 1 × 1 cm. A slide with a solution of zinc salt on it was inserted into the plasma chamber. Next, a vacuum pump was switched on and the system was washed by argon for about 10 s, after which the argon balloon was closed and a vacuum was created inside the plasma chamber. A microwave oven was then activated and a glowing plasma appeared. A typical reaction time was 60 s, although reactions of 10 to 120 s have also been carried out. The resulting product was a Parylene−glass slide coated with zinc oxide. The morphological nature of the coating depends on the zinc salt, the zinc-salt concentration in an ethanol solution, and the reaction time.

Characterization. The X-ray diffraction (XRD) pattern of the product was measured with a Bruker AXS D* advance powder X-ray diffractometer (using Cu Kα radiation =1.5418). The morphology of the glass surface coated with ZnO nanoparticles was measured with a JEOL-JSN 7000F high-resolution scanning electron microscope (HR-SEM) operating at a 15 kV accelerating voltage.

Rutherford Backscattering Spectroscopy (RBS). Microbeam analysis is performed with a 3.0 MeV He^+ beam generated by a Tandetron 1.7 MV accelerator of High Voltage Engineering Europe. The conditions of RBS analysis on the microbeam scanning system (model OM 2000, Oxford Micro beams, Ltd.) are spatial resolution about 2 μm, current density 1 nA, mapping area 500 × 500 μm^2.

The transmission optical spectra were recorded on a CARY 100 Scan UV spectrometer covering a wavelength region from 200 to 800 nm.

Antibacterial Test (18). The antibacterial activity of the coated glass was tested against the Gram-negative *Escherichia coli* (*E. coli*; strain 1313), as well as against the Gram-positive *Staphylococcus aureus* (*S. aureus*; strain 195) bacteria. Both strains were obtained from the Bacteriological Laboratory of the Meir Hospital, Kfar Sava, Israel. A typical procedure was as follows: a nutrient agar (Difco, Detroit, MI) was poured into disposable sterilized Petri dishes and allowed to solidify. Cultures of the bacteria were grown overnight on the nutrient agar. In the morning of the experiment, these cultures were transferred into a flask containing a nutrient broth (NB) at an initial optical density (OD) of 0.1 at 660 nm and allowed to grow at 37 °C with aeration. When the cultures reached an optical density of 0.3 OD at 660 nm (the beginning of the logarithmic phase), they were centrifuged and washed twice with a saline solution (NaCl 0.145 M) at pH 6.5 to yield a final bacterial concentration of approximately 1 × 10^8 CFU mL^{-1}. Square pieces (1 cm ×1 cm) of a ZnO-coated glass slide were placed in a vial (with an inner diameter of 2.5 cm) containing 4.5 mL of saline. The strain cells were then pipetted (500 μL) into the vial. The initial bacterial concentration in the vial was approximately 1 × 10^7 CFU mL^{-1}. To ensure that any decrease in bacterial number was likely to be due to exposure to a coated-glass treatment, two controls were included in the experiment, one with the absence of bacteria and a coated glass (negative control), and the second with the bacteria at the appropriate concentration in saline together with uncoated glass slides (positive control). The bacterial suspensions were incubated and shaken on a rotary platform at 180 shakes min^{-1} and 37 °C for up to 4 h. Samples of 100 μL each were taken at a specified time, diluted 10-fold in saline, and were then streaked uniformly over each nutrient agar plate (Difco). The plates were incubated for 24 h at 37 °C and then counted for viable bacteria. The viable bacteria were monitored with a colony counter by counting the number of colony-forming units from the appropriate dilution on nutrient agar plates. The survival fraction, N/N_0, was determined by calculating the colony-forming units per mL of the culture. The term N_0 stands for the number of colony-forming units at the beginning of the treatment before adding the coated glass, and N is the number of colony-forming units after the treatment for the indicated time of each sample. The bacteriological experiments were repeated three times and the results were found to be reproducible.

RESULTS AND DISSCUSION

The main idea of this paper was to compare three deposition modes: ultrasound irradiation, microwave heating, and microwave plasma, on the basis of morphological film characteristics, and antibacterial properties. The time of the reaction was considered a main factor: we turned from an hourly scale to minutes and to seconds when changing from ultrasound irradiation to microwave heating, and to microwave plasma, respectively.

X-ray Diffraction Characterization. The preliminary characterization of the deposited ZnO nanoparticles on the Parylene glass slides was performed by XRD, as presented in Figure 2. This figure depicts three representative patterns of ZnO-coated Parylene glass by means of (a) 2 h of sonication, (b) microwave irradiation, and (c) a microwave-plasma method using zinc nitrate as a precursor. Miller indices are assigned to the corresponding atomic planes. As can be seen from Figure 2, in all three cases pure ZnO was deposited on the substrate. However, clear differences could still be observed among the three samples. By using sonication, it is possible to deposit large amounts of highly crystalline ZnO on the surface of Parylene-coated glass. The ZnO peaks perfectly match the powder diffraction file (PDF): 01−075−0576, as shown in Figure 2a. It is worth noting that the peaks are sharp, meaning that the ZnO crystallites are

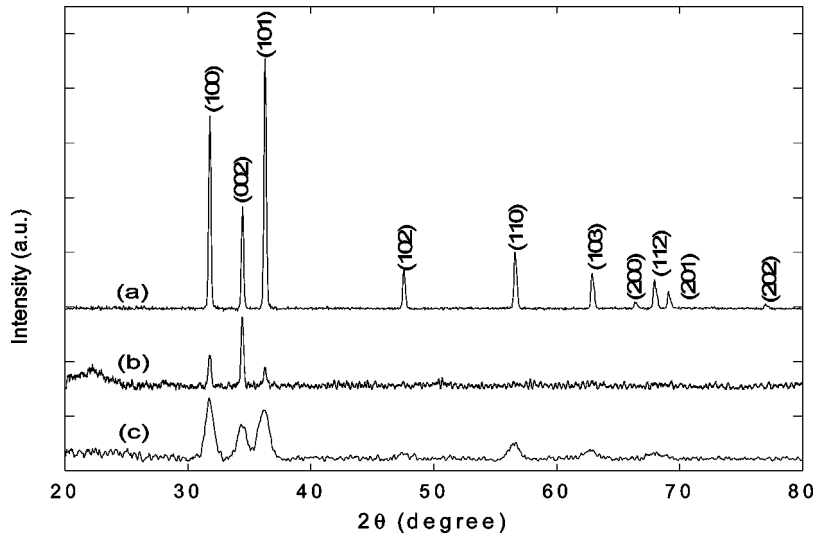

FIGURE 2. XRD pattern of ZnO deposited on a Parylene−glass substrate by means of (a) sonication, (b) microwave irradiation, and (c) a microwave-plasma method. Miller indices are matched to the peaks of the corresponding atomic planes.

not in the small nanometric range. Figure 2b shows the XRD of ZnO deposited on Parylene-coated glass by using microwave irradiation. As can be deduced from the SEM measurements that will be presented further on in this paper, the amount of deposited ZnO by using microwave irradiation is lower. Therefore, the peaks are not as intense as those obtained sonochemically. The broad peak at $2\theta = 22-23°$ can be attributed to the amorphous Parylene layer that was not covered by a sufficient amount of ZnO. In our previous work, we showed that polymers cannot be coated by a large amount of ZnO when using microwave irradiation (11). Figure 2b can also indicate the existence of a preferred orientation growth along the (001) axis because the intensity of the (002) plane is larger than its intensity at PDF 01−075−0576 as well as that of all the other diffractions. In contrast to sonication and somewhat to microwave irradiation that did not yield small ZnO nanoparticles, the microwave-plasma method yielded small nanosized ZnO particles when coating the Parylene-glass plate. As depicted in Figure 2c, related to the microwave-plasma process, the X-ray diffraction profile matches well with the PDF 01−075−0576. It can be clearly observed that peaks of ZnO received by the microwave-plasma method are much broader than the peaks received by the other two methods. Using the Scherrer equation, the sizes of ZnO nanoparticles are roughly estimated to be in the range of 15 nm.

Coating Mechanism. The sonochemical and microwave synthesis of ZnO, as well as coating mechanisms of both methods on rigid surfaces, were previously described and will not be repeated here (7, 9, 11). As for microwave plasma, a paper dealing with the mechanism has recently been submitted for publication. Briefly, when the plasma is activated, all surfaces, including zinc precursors, absorb electrons from plasma, thus forming a sheath that prevents any additional penetration of electrons from the plasma, but attracts positively charged species (Ar^+) that hit the zinc precursors with a high energy. These collisions, together with the collective collisions inside plasma, are responsible for the increase in the temperature inside the plasma chamber, and the zinc precursors are thermally decomposed to form ZnO. The charged surface of ZnO is labeled as $[ZnO]^{n-}$ (scheme 1).

$$\begin{aligned} &Ar + e^- \xrightarrow{MW} Ar^+ + 2e^- + \Delta \\ &Zn(NO_3)_2 \xrightarrow{EtOH} Zn(OH)(NO_3) \xrightarrow{e^-,\Delta} [ZnO]^{n-} + \\ &\quad NO_2 + 1/4O_2 + 1/2H_2O \end{aligned} \qquad (1)$$

It should also be emphasized that all of the coating products were stable and could not be removed from the surface by a simply washing with water, or ethanol and/or acetone. The methods we used for the leaching examination were dynamic light scattering (DLS) and transmission electron microscopy (TEM). After placing the coated glasses in each of the above-mentioned solvents for duration of 7 days, the DLS and TEM studies did not reveal the presence of any nanoparticles in the leaching solution. That means that the deposited ZnO nanoparticles are strongly anchored to the Parylene substrate.

Morphology Examination. Morphologies of the ZnO films deposited on the Parylene−glass surfaces were studied by HR-SEM. Using the three methods of deposition, several images were detected (Figures 3a−h). Images a and b in Figure 3 depict the ZnO films obtained by ultrasound irradiation of 1 and 2 h, respectively. For sample a, where the deposition process lasted 1 h, a dense layer of undetermined particle shape is observed enriched with some distinct nanoparticles. Increasing the reaction time to 2 h (sample b) enabled the formation of aggregated particles of up to ∼5 μm in the form of oriented layers. Conducting the deposition process by microwave heating required a shorter reaction time, and resulted to the formation of ZnO layers consisting of smaller nanoparticles of ∼100 nm (samples c and d). Using microwave plasma shortened the reaction time to 60 s with the very unique deposition of very small ZnO nanoparticles. Using zinc acetate as the precursor yielded ∼25 nm size particles (samples e, f), and when using zinc nitrate as

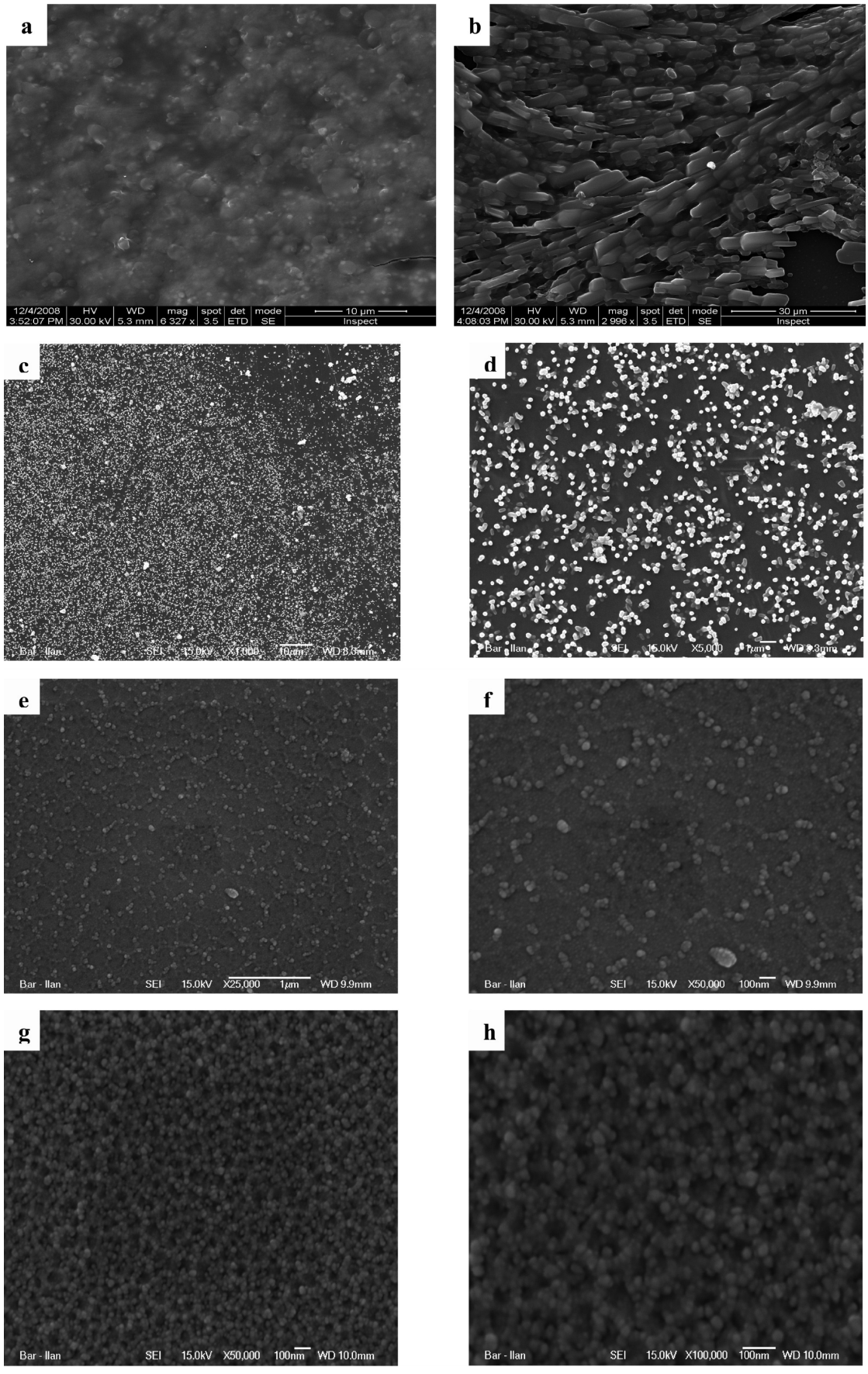

FIGURE 3. HR-SEM of ZnO films on Parylene−glass deposited by: (a, b) ultrasound irradiation for 1 and 2 h respectively; (c, d) microwave heating for 5 min (the bar of c is 10 μm and that of d is 1 μm); (e, f) microwave-plasma using zinc-acetate as a precursor (the bar of e is 1 μ and that of f is 100 nm); (g, h) microwave plasma using zinc-nitrate as a precursor (the bars are 100 nm).

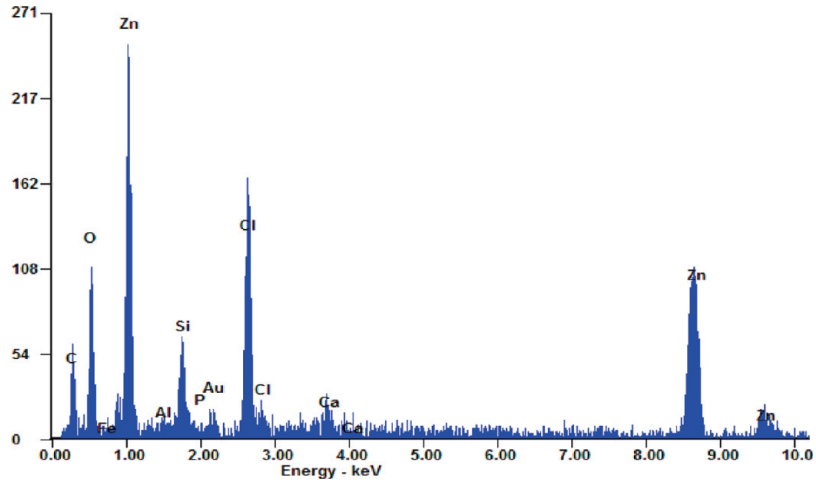

FIGURE 4. EDS. X-ray elemental spectra of Parylene glass coated with ZnO by microwave. C and Cl peaks are from the Parylene, Si from the glass, Au originates from the grid coating.

the precursor a multilayer of ~27 nm (sample g and h) particles is observed. It can be concluded from these images that turning from ultrasound irradiation as the deposition process to microwave heating and to microwave plasma is associated with a significant decrease in the reaction time. This decrease is an important factor for creating uniform films of small nanoparticles. It should be noted that for the three above-mentioned coating routes no visible damage to the Parylene structure could be observed. Regarding the difference of the coating structures obtained by the acetate and the nitrate precursors, we suggest that stronger interactions between the solvated acetate groups of the ZnO precursor and the polymer surface results in a horizontal localization of the precursor on the surface, and therefore the newly formed ZnO coating is of a one-layer thickness.

Energy-dispersive X-ray spectroscopy (EDS) is an analytical technique, coupled to the HR-SEM, used for the elemental analysis. The existence of zinc on the Parylene-glass surface was detected by the EDS. Figure 4 depicts the EDS of the microwave-coated product. The figure is also characteristic of all three products from the different deposition routes. No signal of Zn was detected for the uncoated Parylene glass (data not shown).

Depth Profile. RBS is an analytical nuclear technique to quantitatively determine depth profiles of elemental concentration. The RBS method was utilized to compare the penetration depth of the ZnO nanoparticles deposited by the above-mentioned modes. The RBS technique is based on elastic collisions between ions and the atomic nucleus. The slowing down of ions in matter provides depth resolution. The analysis was performed on ZnO-coated Parylene glass by means of (a) 2 h of sonication, (b) microwave irradiation, and (c) a microwave-plasma method using zinc nitrate as a precursor. From the analysis results (Figure 5), the following can be concluded: (1) Whatever the deposition method used, a ZnO coating layer is present, but variations in the ZnO thickness are observed. (2) The deepest penetration occurs when sonochemistry is applied (above 1000 nm) and is found to be better than the microwave and the microwave-plasma deposition modes (Figure 5a,b). (3) The highest

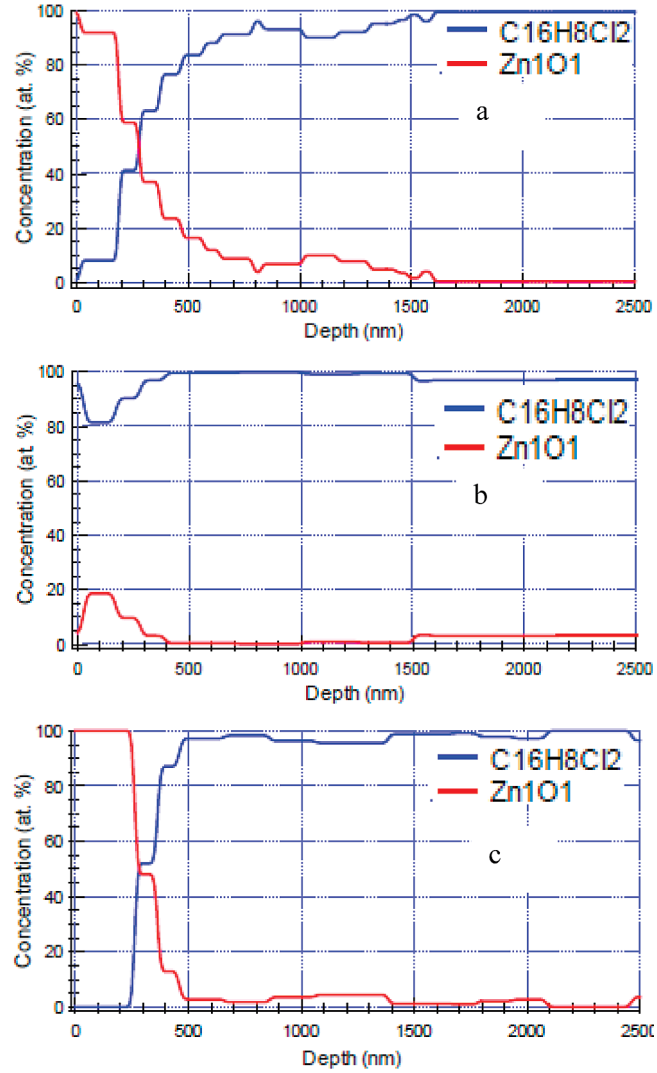

FIGURE 5. RBS of Parylene glass coated with ZnO by three coating modes: (a) sonochemistry, (b) microwave, (c) microwave-plasma. The layer thicknesses are in units of nanometer. No signal of ZnO was detected for the uncoated Parylene glass (data not shown).

concentration of coated ZnO in the upper layers (up to 250 nm) of the Parylene-coated glass is obtained using the microwave-plasma method (Figure 5c). It also appears that

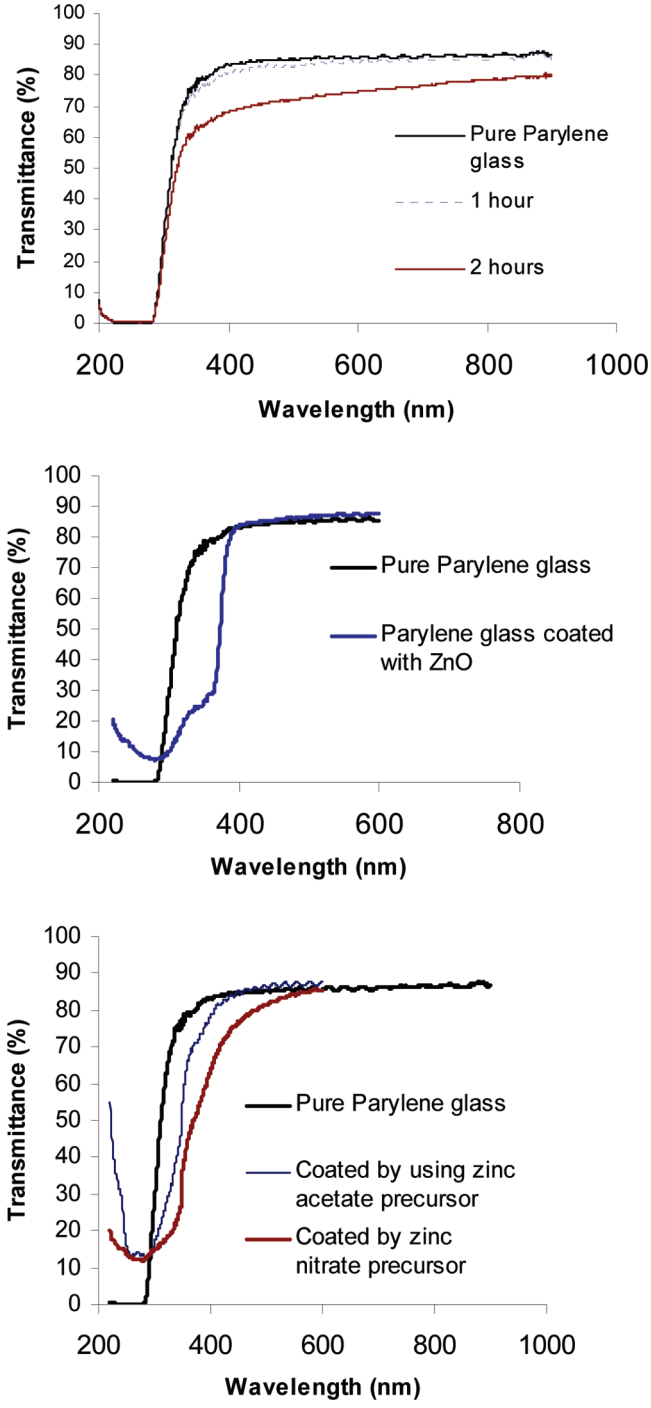

FIGURE 6. (a) Spectral transmittance of deposited Parylene glass by ultrasound irradiation, (b) spectral transmittance of deposited Parylene glass by microwave heating, (c) spectral transmittance of deposited Parylene glass by microwave plasma.

among the three coating routes, the adherence of the upper ZnO layers of the microwave product to the substrate surface is the weakest; therefore, the upper coating is less detectable by the RBS (Figure 5b).

Optical Properties. To investigate the optical properties of the deposited ZnO particles on the Parylene-glass substrates, transmittance spectra were carried out. A decrease in the transmittance, with an increase in the reaction time, was observed for the ultrasound coating (Figure 6a). Unlike the ZnO films deposited by 2 h ultrasound irradiation, the ZnO-loaded Parylene-glass samples obtained by microwave and microwave plasma appear relatively more transparent and without cords (inhomogeneous in density) visible to a naked eye. Figure 6b shows the transmittance spectrum of deposited Parylene-glass substrate obtained by a microwave heating process. The figure shows a clear decrease of the transmittance of the ZnO coating products in the visible region (and NIR) light (400−800 nm) as well as a decrease of transmittance in the UV region. In Figure 6c the transmittance of the microwave plasma products obtained by the two precursors are compared. It can be seen that transmittance for the nitrate precursor is lower than the transmittance for the acetate precursor in the wavelength of 300−600 nm (Figure 6c). Yet, pure Parylene glass has the highest transmittance (up to 90%).

Antibacterial Activity. The antibacterial activity of Parylene-glass slides coated with ZnO via ultrasonic, microwave, and microwave-plasma irradiation was studied. Due to the limited paper length, we will demonstrate only the results for a representative sample of each reaction route (sample b, sample e, sample g, as coded above in Figure 3). These samples were tested against the Gram negative bacterium *E. coli* and against the Gram positive bacterium *S. aureus*. The viable bacteria were monitored by counting the number of colony-forming units (CFU). The incubated time of the bacteria with pure glass slides or with glass slides coated solely with Parylene in the saline solution was examined. No effect on the viability of the bacteria is observed for both the pure glass and the glass-coated Parylene, even after 4 h of incubation. As shown in Table 1, bacteriological treatment for 1 h with sample b (sonochemistry product) resulted in a 52% reduction in *E. coli* viability and a 25% reduction in *S. aureus* viability. Three hours of treatment resulted in the complete inhibition of *E. coli* growth and a 76% reduction in *S. aureus* viability. A test with sample e (microwave product) resulted in the almost complete reduction of *E. coli* growth even after 1 h of treatment. In addition, the antibacterial effect against *S. aureus* was also slightly improved. Hence, although the surface concentration of ZnO is lower in the microwave product (as revealed by RBS), it appears that the decreased particle size is a more critical factor in the antibacterial action. However, sample g (microwave-plasma product) has shown remarkably improved antibacterial properties against both strains. It appears that the factor of reducing the particle size to a small nanometric scale enhances the antibacterial activity (see ref 4). This factor may outweigh the variability of the coating concentrations. As we pointed out above, we have recently found that the major components responsible for the bactericidal effect of ZnO nanoparticles were some species of oxyradicals in the solution, mainly hydroxyl radicals. These reactive-oxygen-species (ROS) were detected in electron spin resonance (ESR) studies. The difference in the antibacterial action of ZnO-coated Parylene glass upon the two strains of bacteria can be explained in light of the difference in their susceptibility toward ROS. In this respect, it was recently found that *S. aureus* bacterium contains a large amount of

Table 1. Antibacterial Activity Test of the Coated Glass Slides Against *E. coli* and *S. aureus*; Viable Bacteria Were Monitored by Counting the Number of Colony-Forming Units (CFU) and N/N_0 is Survival Fraction

		E. coli			*S. aureus*		
sample	duration of treatment (h)	CFU mL^{-1}	N/N_0	% reduction in viability	CFU mL^{-1}	N/N_0	% reduction in viability
sonochemistry	0	6.6×10^7	1	0	6.3×10^7	1	0
	1	3.2×10^7	4.8×10^{-1}	52	4.7×10^7	7.5×10^{-1}	25
	3	4.2×10^2	7.0×10^{-6}	~100	1.5×10^7	2.4×10^{-1}	76
microwave	0	6.6×10^7	1	0	6.3×10^7	1	0
	1	2.5×10^7	3.9×10^{-1}	61	4.4×10^7	6.9×10^{-1}	31
	3	3.1×10^2	4.7×10^{-6}	~100	1.1×10^7	1.7×10^{-1}	83
microwave- plasma	0	6.6×10^7	1	0	6.3×10^7	1	0
	1	1.3×10^6	2.0×10^{-2}	98	6.9×10^6	1.1×10^{-1}	89
	3	2.1×10^2	3.2×10^{-6}	~100	1.9×10^6	3.0×10^{-2}	97

carotenoid pigments, rendering its higher resistance to oxidative stress (19).

CONCLUSION

The growing demand for a new generation of antimicrobial materials calls for novel fabrication technologies for efficient disinfection, microbial control products, food equipment, domestic cleaning services, etc. Rigid antibacterial matrices such as coated glass provide an innovative solution for any environment where high standards of hygiene are necessary. This includes: fighting against airplane- and hospital-caught infections, deodorizing, and air-purification functional coating. Thus, antibacterial Parylene-glass coatings can come to our aid in reducing the sterilization cost and manual hours for disinfection of the surrounding domains. Moreover, by utilizing different thicknesses of the ZnO coatings, such properties can be integrated with UV protection and controlling light transmittance.

Our objective in this investigation was to compare three deposition modes, all of which are simple one-step synthesis and coating routes—ultrasound irradiation, microwave heating, and microwave plasma—for their morphological, optical, and biocidal properties. All ZnO products obtained by these methods were finely dispersed on the Parylene-glass surface without significant damage to the Parylene structure. However, it appears that among these reaction routes the microwave plasma yielded significant advantages with respects to the shortening the reaction time, decreasing the particle size of the ZnO down to the nanometric scale, and obtaining the largest amount of ZnO nanoparticles on the surface. Reducing the ZnO particle size also results in improving the antibacterial effect of the coated product. On the other hand, the deepest penetration of the ZnO nanoparticles into the Parylene layer was obtained by the sonochemical method. This is explained by the driving force of the microjets, which throw the newly formed nanoparticles at the surface at a very high speed. This enables the nanoparticles to penetrate deeply into the Parylene. Such a trait may be of advantageous in terms of stability and prolonging the shelf life of the coated Parylene glass as a commercial product.

Acknowledgment. This work was partially supported by the European Project MULTIPOL under Contract FP6-NMP4-STREP 033201. The deposition of the Parylene was performed at HES-SO Arc on a Parylene deposition reactor lent by COMELEC SA. We thank the COMELEC company for lending the equipment.

REFERENCES AND NOTES

(1) Xiong, M. N.; Gu, G. X.; You, B. J. *Appl. Polym. Sci.* **2003**, *90*, 1923–1931.
(2) Tang, E.; Cheng, G.; Pang, X.; Ma, X; Xing, F. *Colloid Polym. Sci.* **2006**, *284*, 422–428.
(3) Sawai, J. *J. Microbiol. Methods* **2003**, *54*, 177–182.
(4) Applerot, G.; Lipovsky, A.; Dror, R.; Perkas, N.; Nitzan, Y.; Lubart, R.; Gedanken, A. *Adv. Funct. Mater.* **2009**, *19*, 842–852.
(5) Hozumi, A.; Kojima, S.; Nagano, S.; Seki, T.; Shirahata, N.; Kameyama, T. *Langmuir* **2007**, *23*, 3265–3272.
(6) Lee, K. H.; Huang, K. H.; Tseng, W. L.; Chiu, T. C.; Lin, Y. W.; Chang, H. T. *Langmuir* **2007**, *23*, 1435–1442.
(7) Perelshtein, I.; Applerot, G.; Perkas, N.; Wehrschuetz-Sigl, E.; Hasmann, A.; Guebitz, G.; Gedanken, A. *Surf. Coat. Technol.* **2009**, *204*, 54–57.
(8) Gedanken, A. *Ultrason. Sonochem.* **2004**, *11* (2), 47–55.
(9) Kotlyar, A.; Perkas, N.; Amiryan, G.; Meyer, M.; Zimmermann, W.; Gedanken, A. *J. Appl. Polym. Sci.* **2007**, *104*, 2868–2876.
(10) Gabriel, C.; Gabriel, S.; Grant, E. H.; Halstead, B. S. J.; Mingos, D. M. P. *Chem. Soc. Rev.* **1998**, *27*, 213–223.
(11) Irzh, I.; Gedanken, A. *J. Appl. Polym. Sci.* **2009**, *113*, 1773–1780.
(12) Irzh, A.; Genish, I.; Chen, L.; Ling, Y. C.; Klein, L.; Gedanken, A. *J. Phys. Chem. C* **2009**, *113*, 14097–14101.
(13) Vollath, D. In *Nanomaterials*; Wiley-VCH, Weinheim, Germany, 2008.
(14) Fortin, J. B.; Lu, T. M. *Chem. Mater.* **2002**, *14*, 1945–1949.
(15) Lin, H. K.; Zheng, S.; Balic, M.; Tai, Y. C.; Datar, R. H.; Cote, R. J. *Proceedings of the 97th Annual Meeting of the American Association for Cancer Research*; Washington, D.C., April 1—5, 2006; American Association for Cancer Research: Philadelphia, PA, 2006; Vol. 47, Meeting Abstracts 1207-b.
(16) Jiang, F.; Han, Z.; Wang, X. Q.; Tai Y. C. U.S. Patent 6 511 859, 2003.
(17) Fearnot, N. E.; Kozma, T. G.; Ragheb, A. O.; Voorhees, W. D U.S. Patent 5 609 629, 1997.
(18) Nitzan, Y.; Balzam-Sudakevitz, A.; Ashkenazi, H *J. Photochem. Photobiol., B* **1998**, *42*, 211–218.
(19) Liu, G. Y.; Essex, A.; Buchanan, J. T.; Datta, V.; Hoffman, H. M.; Bastian, J. F.; Fierer, J.; Nizet, V. *J. Exp. Med.* **2005**, *202*, 209–215.

AM900825H